Available online at www.sciencedirect.com

ScienceDirect

Scripta Materialia 75 (2014) 10–13

Scripta MATERIALIA

www.elsevier.com/locate/scriptamat

Discerning size effect strengthening in ultrafine-grained Mg thin films

J.A. Sharon,[a,b] Y. Zhang,[b] F. Mompiou,[c] M. Legros[c] and K.J. Hemker[b,*]

[a] *Sandia National Laboratories, Albuquerque, NM, USA*
[b] *The Johns Hopkins University, Baltimore, MD, USA*
[c] *CEMES–CNRS & Université de Toulouse, Toulouse, France*

Received 8 June 2013; accepted 16 October 2013
Available online 23 October 2013

Microtensile experiments have been performed to elucidate the mechanical response of ultrafine-grained Mg thin films. Strengths of 160 MPa and elongations up to 8% were measured. Post-deformation electron microscopy indicates a lack of intragranular dislocation confinement. While strength does increase with decreasing grain size, the size effect for hexagonal Mg is not as strong as that reported for face-centered cubic metals. Strength appears to be governed by a lack of dislocation pile-up as well as texture and Peierls effects.

Keywords: Size effect; Mechanical properties; Hall–Petch strengthening; Hexagonal; Thin films

Due to its low density, magnesium has garnered much attention as a potential metal for lightweight aerospace and automotive components [1]. Reductions in grain size should benefit the design of Mg-based alloys by providing Hall–Petch [2,3] strengthening and potentially activating grain-boundary (GB)-mediated mechanisms that could enhance deformability [4]. Size effects at the submicron level have been widely studied for face-centered cubic (fcc) metals but investigations of hexagonal close-packed (hcp) systems are still relatively nascent. Work on Ti pillars by Norfleet [5] measured a weak size effect in the micron regime, suggesting that the confinement of dislocations provided less stress enhancement than the Peierls stress [6,7] needed to move dislocations through the lattice. A similar trend was found in body-centered cubic (bcc) metals [8,9] with the strong Peierls friction metals exhibiting lower size effects. This work seeks to elucidate the size-specific mechanical properties of ultrafine-grained (ufg) Mg free-standing thin films.

Test specimens were prepared by depositing Mg onto a Si platform patterned with a tensile geometry following the process outlined in Refs. [10] and [11]. The films were synthesized using electron beam evaporation from a 99.999% pure source. The deposition was pulsed; at a base pressure of 4×10^{-7} Torr, six 33 nm deposition steps each separated by 1 min dwells were repeated to build a nominally 200 nm thick film. Measurements with a stylus tip profilometer revealed that the actual film thickness was 250 ± 10 nm. Prior to testing, the films were made free standing by removing the Si under the gauge region with a dry gas etch of XeF_2. Mechanical testing was conducted using a small-scale tensile apparatus described in Ref. [12]. The system was outfitted with a 10 g load cell and the experiments were displacement controlled using a linear actuator with 30 nm step resolution. Specimens were gripped using UV-curable adhesive, and alignment prior to permanent bonding was performed optically with a stereoscope, adjusting the sample position with a five-axis motorized stage. All tensile tests were conducted at an initial specified strain rate of 5×10^{-4} s^{-1}. Strain was measured using digital image correlation processed with a MATLAB®-based code [13].

Analysis of the as-deposited Mg by transmission electron microscopy (TEM, Phillips 420) found the grains to be essentially free of dislocations and growth twins. The area-weighted as-deposited grain size was 197 nm with an 89 nm standard deviation, putting the Mg in the ufg regime. An amorphous oxide has been reported to form on scratched Mg films [14] and the Mg of this

* Corresponding author at: Johns Hopkins University, Baltimore, MD, USA. Tel.:+1 410 516 4489; e-mail: hemker@jhu.edu

1359-6462/$ - see front matter © 2013 Acta Materialia Inc. Published by Elsevier Ltd. All rights reserved.
http://dx.doi.org/10.1016/j.scriptamat.2013.10.016

study did have some small amorphous pockets, most likely oxide, randomly dispersed amongst the grains. As Mg is anisotropic [15], an out-of-plane orientation map to discern texture was measured using a Phillips CM20 field emission gun transmission electron microscope equipped with a NanoMEGAS orientation mapping unit. A 4 μm × 4 μm scan, given in Figure 1a, shows the orientation distribution of the grains. The 0001 pole figure (Fig. 1b), which reveals the basal texture, indicates that ~9.5% of grains are positioned with their basal plane parallel to or within 10° of the film surface.

The stress–strain responses from five tensile experiments are recorded in Figure 2. All specimens exhibited similar behavior; each yielded at around 131 MPa, reached a peak stress near 160 MPa, and then strained to failure without significant hardening. Elongation at fracture varied from 3% to 8%. Specimens A and B failed prematurely and this was attributed to an undetected edge flaw. The other specimens failed via necking with local strain levels of the order of 13–15% inside the neck.

Post-fracture TEM analysis was conducted and a representative image of the deformed Mg is provided in Figure 3. Only a very small fraction of the grains contained dislocations. Experiments and simulations suggest that small grain metals exhibit GB-mediated flow mechanisms such as GB dislocation emission [16,17], sliding [18] or coupled migration [19]. The area-weighted grain size of the deformed Mg was 188 nm with a 76 nm standard deviation. While smaller than the as-deposited grain size, in statistical terms no refinement occurred. As coarsening due to GB coupling is not detected, deformation is most likely occurring through dislocation or twin emission and absorption at GBs. Simulations on small-grain Mg also suggest this deformation mode with dislocation and twin emission reported to occur at GBs [20,21]. Deformation twins were found in a small fraction of the grains. The observed twinning system was (10–11) <10–12> (see Fig. 3 inset) which occurs in crystallites whose c-axis contracts. This compression twinning (CT) is recognized in hcp systems [22] and has been reported in single-crystal Mg experiments on bulk [23] and nanoscale [24,25] specimens but is absent in

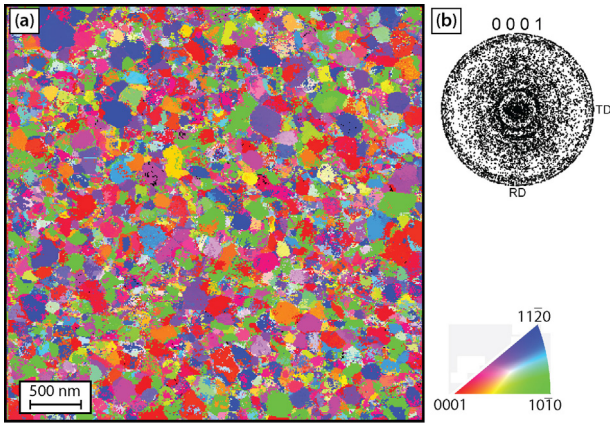

Figure 1. (a) Out-of-plane orientation map of as-deposited Mg with (b) corresponding 0001 pole figure.

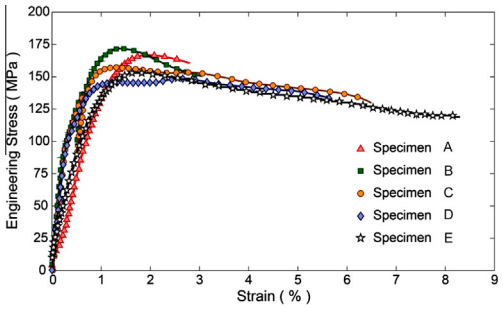

Figure 2. Tensile response data for 250 nm thick free-standing Mg thin films.

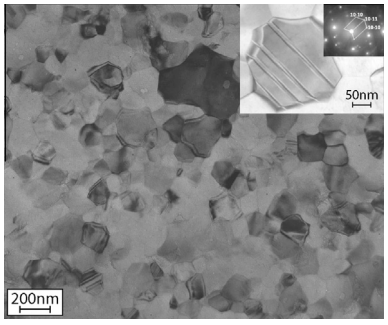

Figure 3. Representative bright-field TEM image of deformed Mg with image of a compression twin inset.

micron-size samples [26,27]. Tensile twinning (TT), which occurs when the c-axis of a grain extends, was not widely detected. GB sliding was not confirmed here but other studies [4,28] suggest that this mechanism may be active.

A Hall–Petch plot (Fig. 4a) was assembled using data extracted from published studies [28–33] to see how yield strength (σ_y) varied with the inverse square root of grain size (d). Mg appears to follow the Hall–Petch trend until d = 1 μm where, as noted by Choi et al. [28], a decrease in the strengthening slope occurs. Curiously, σ_y for the present study is exceptionally low as some of the reference data for grain sizes larger than 1 μm have higher yield strengths.

To better understand why such a low yield stress is measured in the ufg Mg, the overarching Hall–Petch constructs were first considered. The strengthening is chiefly based upon dislocation pile-up, and in ufg Mg there is a clear lack of intragranular dislocation storage (see Fig. 3). If no pile-up occurs, the strengthening trend is not likely to be followed. Furthermore, Hall–Petch assumes a $\sigma_y \propto d^{-0.5}$ relationship which may not be valid [34]. If d vs. σ_y is plotted as in Figure 4b, it is seen that smaller grains are associated with higher yield points, but the breakdown of the strengthening slope is not as evident. A power-law fit to the individual data sets reveals that the size effect ranges from $d^{-0.1}$ to $d^{-0.35}$ which is less than $d^{-0.5}$ and also less than the $d^{-0.6}$–d^{-1} size effect found in fcc single-crystal experiments [35]. Three fits are provided in Figure 4b and fits for all data sets are denoted in the legend. The values are in line with those measured for bcc metals [8,9] from single-crystal pillar experiments by Schneider et al., who

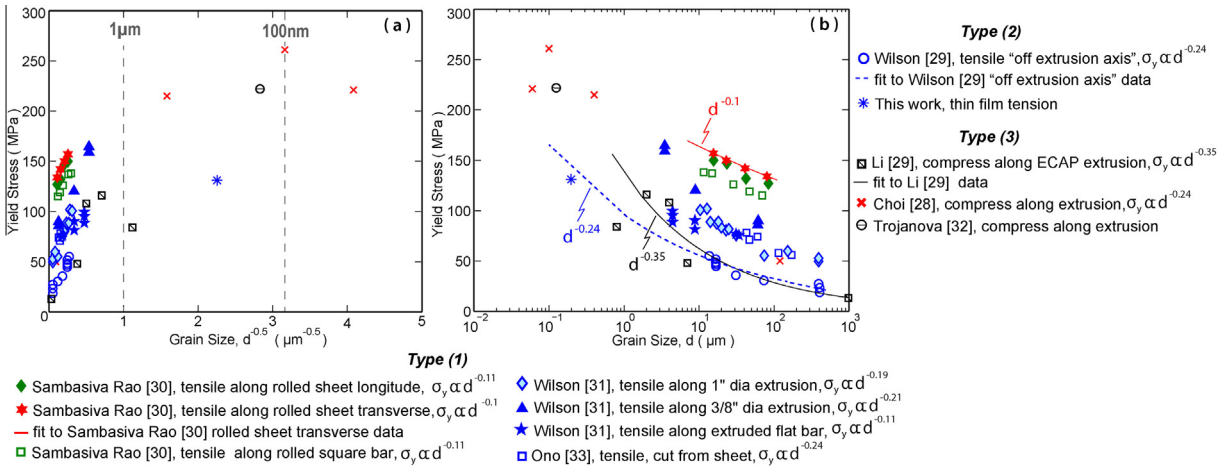

Figure 4. (a) Hall–Petch plot and (b) grain size vs. yield strength for polycrystalline Mg. Data have been estimated from published studies; differences may exist in how each of these studies defined the yield point. See text for an explanation regarding the different types of Mg as grouped in the legend.

attributed the reduced size effect in bcc metals to a high Peierls stress. As suggested by Gröeger and Vitek [36], it is proposed that the low mobility of screw dislocations due to the Peierls barrier in bcc metals results in a back stress on dislocation sources that encumbers their operation.

In situ TEM studies of prismatic slip in Mg by Couret and Caillard [6,7] showed fast movement of non-screw segments under stress, whereas screw dislocations were slower. Slow screw dislocations suggest a non-planar spreading of cores, resulting in a Peierls effect akin to bcc metals [8,9,36]. Atomistic studies of hcp metals by Vitek and Igarashi [37] also indicate that, for prismatic slip, the dislocation core spreads out of plane; however, not all slip systems are Peierls limited to the same degree. The effect on basal slip in Mg is lower as the dislocation cores are relatively more planar. Mg micropillars tested along various orientations demonstrate that lattice friction can significantly hinder size effects [38].

As different slip systems are subject to different amounts of Peierls barrier, how σ_y varies with d will be sensitive to texture and loading condition. Texture, albeit under the assumption that $\sigma_y \propto d^{-0.5}$, has been reported to impact grain size strengthening in Mg [30,39]. In pure bulk Mg, the softest mechanisms to activate are basal slip at less than 1 MPa [40] and TT that occurs at less than ~10 MPa [41]. Harder mechanisms include pyramidal slip [42], prismatic slip [43] and CT [44], which are all estimated to require >30 MPa to activate. In general, Mg's basal planes align parallel to the processing direction. The data presented in Figure 4 can then be grouped into three types: (1) basal texture tested in tension with the c-axis of basal grains contracting such that deformation is via CT, pyramidal and prismatic slip; (2) weak/random texture with a fraction of the grains able undergo easy basal slip and TT; and (3) basal texture tested in compression with the c-axis of basal grains extending thus allowing TT.

For type (1) Mg, yielding will be controlled by CT, pyramidal and prismatic slip. As these slip systems are Peierls limited, a low size effect is expected. The type (1) Mg tested by Sambasiva Rao and Prasad [30] and Wilson and Chapman [31] had, on average, a size effect of $\sigma_y \propto d^{-0.11}$ and $\sigma_y \propto d^{-0.17}$, respectively. These are indeed lower in comparison to the Mg of the other types. The type (1) Mg by Ono et al. is slightly higher with $\sigma_y \propto d^{-0.24}$ but this may be due to weak texture as no orientation analysis is provided in Ref. [33].

For type (2) Mg, lower yield points are expected as the weak texture allows basal slip and TT to operate. Since basal slip has lower Peierls effects, a relatively stronger size effect should be present. A notable size effect for basal slip and TT in Mg has been observed in in situ TEM nanopillar compression experiments by Ye et al. [45]. Consider Wilson and Chapman's [31] type (1) data for 1 in. diameter extrusions compared to their data on weakly textured "off extrusion axis" specimens. At $d = \sim 14$ μm (see Fig. 4b), the "off extrusion axis" samples yield at 55 MPa, while the Mg loaded along the extrusion direction yields closer to 89 MPa, a 38% reduction in strength. As for the size effect, "off extrusion axis" Mg is indeed more sensitive to grain size with $\sigma_y \propto d^{-0.24}$. Interestingly, the weakly textured ufg Mg of this study broadly fits the $d^{-0.24}$ strengthening trend denoted by the dashed blue line in Figure 4b. This observation suggests that the yield strength of the ufg Mg is not anomalously low as it appears in Figure 4a and that grain size may not be the dominant factor in controlling strength.

The type (3) Mg, governed by easy TT, will have relatively low yield points. In addition, as twinning can have a larger strengthening effect with decreasing grain size compared to that of slip [46], a higher size effect is expected. The data sets for type (3) Mg come from the work of Choi et al. [28], where $\sigma_y \propto d^{-0.24}$, and that of Li et al. [29], where $\sigma_y \propto d^{-0.35}$ (power-law fits exclude inverse Hall–Petch data points). The value for Choi's [28] Mg is comparable to the "off extrusion axis" data from Wilson and Chapman [31] and may therefore stem from weak texture. The size effect for Li et al.'s [29] Mg is, however, higher as expected.

While the above discussion proposes that a lack of dislocation confinement and Peierls effects overshadow strengthening from grain size reduction, two other

factors, not addressed in detail here, should be considered. First is the impact of impurities, solutes and oxide. Kutsukake et al. [47] suggested that impurities can significantly impact the strength of Mg. Second is the ease of twinning in ufg Mg. Yu et al. [48], proposed that large single crystals easily twin since they are more likely to contain a defect spanning multiple consecutive slip planes to stimulate the passage of partials for twin formation. Nanosize Mg single crystals require hundreds of MPa to twin [24,25], and hence perhaps the GBs of the ufg Mg act as defects lowering the stress for twinning. It is recognized that CT and TT was not prolifically identified in the ufg Mg, but it can be speculated that the activity may have been underestimated. The mechanism would go undetected in post-deformation TEM analysis if entire grains took the twin orientation with no remnant of the twin boundary left behind. While not confirmed in this work, the scenario seems plausible as TT to nearly consume entire pillars in pure Mg [45] and grains [49] in a Mg alloy has been reported.

In summary, Mg does exhibit a Hall–Petch-like trend in the sense that, overall, smaller grains do result in an increased yield point. The size effect is, however, weaker than that reported for fcc metals. TEM observations of the deformed grain structure suggest that the ufg Mg of this study has low grain size strengthening due to its inability to confine dislocations. Furthermore, comparisons to published literature data also indicate that the strength of Mg needs to be considered in the context of texture and Peierls effects.

The authors would like to thank Dr. K. Livi, H. Vo and P. Rottmann for assistance with specimen preparation. This work was supported by the US Department of Energy, Office of Basic Energy Sciences. Final analysis and manuscript preparation by J.A.S., now at Sandia National Laboratories, was supported through a separate grant from the US Department of Energy, Office of Basic Energy Sciences. Sandia National Laboratories is a multi-program laboratory managed and operated by Sandia Corporation, a wholly owned subsidiary of Lockheed Martin Corporation, for the US Department of Energy's National Nuclear Security Administration under contract DE-AC04-94AL85000.

[1] B.L. Mordike, T. Ebert, Mater. Sci. Eng., A 302 (2001) 37–45.
[2] E.O. Hall, Proc. Phys. Soc. Lond. Sect. B 64 (1951) 747–753.
[3] N.J. Petch, J. Iron Steel Inst. 174 (1953) 25–28.
[4] S. Hwang et al., Scripta Mater. 44 (2001) 1507–1511.
[5] D.M. Norfleet, Ph.D. Thesis, The Ohio State University, 2007.
[6] A. Couret, D. Caillard, Acta Metall. 33 (1985) 1447–1454.
[7] A. Couret, D. Caillard, Acta Metall. 33 (1985) 1455–1462.
[8] A.S. Schneider et al., Mater. Sci. Eng. Struct. Mater. Prop. Microstruct. Process. 508 (2009) 241–246.
[9] A.S. Schneider et al., Mater. Sci. Eng. Struct. Mater. Prop. Microstruct. Process. 528 (2011) 1540–1547.
[10] W.N. Sharpe, et al., New Test Structures and Techniques for Measurement of Mechanical Properties of MEMS Materials, 1996.
[11] D.S. Gianola et al., Acta Mater. 54 (2006) 2253–2263.
[12] W.N.S. D.S. Gianola, M. Legros, K.J. Hemker, TMS Letters (2004).
[13] C. Eberl, et al., MATLAB File Exchange Server (2006). http://www.mathworks.com.
[14] J.H. Nordlien et al., Corros. Sci. 39 (1997) 1397–1414.
[15] E.W. Kelly, W.F. Hosford, Trans. Metall. Soc. AIME 242 (1968) 654–661.
[16] H. Van Swygenhoven et al., Phys. Rev. B 66 (2002) 024101-1–024101-8.
[17] K.S. Kumar et al., Acta Mater. 51 (2003) 387–405.
[18] H. Van Swygenhoven, P.A. Derlet, Phys. Rev. B 64 (2001).
[19] F. Mompiou et al., Acta Mater. 57 (2009) 2198–2209.
[20] D.H. Kim et al., Acta Mater. 58 (2010) 6217–6229.
[21] D.H. Kim et al., Mater. Sci. Eng., A 528 (2011) 5411–5420.
[22] J.W. Christian, S. Mahajan, Prog. Mater. Sci. 39 (1995) 1–157.
[23] B. Syed et al., Scripta Mater. 67 (2012) 700–703.
[24] Q. Yu et al., Jom 64 (2012) 1235–1240.
[25] Q. Yu et al., Nano Lett. 12 (2012) 887–892.
[26] C.M. Byer et al., Scripta Mater. 62 (2010) 536–539.
[27] E. Lilleodden, Scripta Mater. 62 (2010) 532–535.
[28] H.J. Choi et al., Mater. Sci. Eng. Struct. Mater. Prop. Microstruct. Process. 527 (2010) 1565–1570.
[29] J. Li et al., Mater. Sci. Eng. Struct. Mater. Prop. Microstruct. Process. 528 (2011) 5993–5998.
[30] G.S. Rao, Y. Prasad, Metall. Trans. Phys. Metall. Mater. Sci. 13 (1982) 2219–2226.
[31] D.V. Wilson, J.A. Chapman, Philos. Mag. 8 (1963) 1543.
[32] Z. Trojanova et al., Mater. Sci. Eng. Struct. Mater. Prop. Microstruct. Process. 483–84 (2008) 477–480.
[33] N. Ono et al., Mater. Lett. 58 (2004) 39–43.
[34] D.J. Dunstan, A.J. Bushby, Int. J. Plast. 40 (2013) 152–162.
[35] M.D. Uchic et al., Annu. Rev. Mater. Res. 39 (2009) 361–386.
[36] R. Groeger, V. Vitek, Philos. Mag. Lett. 87 (2007) 113–120.
[37] V. Vitek, M. Igarashi, Philos. Mag. A 63 (1991) 1059–1075.
[38] K.G. Seok, Ph.D. Thesis, Université de Grenoble, 2011.
[39] W. Yuan et al., Scripta Mater. 65 (2011) 994–997.
[40] A. Akhtar, E. Teghtsoonian, Acta Metall. 17 (1969) 1339–1349.
[41] E.W. Kelley, W.F. Hosford, Trans. Metall. Soc. AIME 242 (1968) 5–13.
[42] T. Obara et al., Acta Metall. 21 (1973) 845–853.
[43] A. Akhtar, E. Teghtsoonian, Acta Metall. 17 (1969) 1351–1356.
[44] B.C. Wonsiewicz, Ph.D. Thesis, Massachusetts Institute of Technology, 1966.
[45] J. Ye et al., Scripta Mater. 64 (2011) 292–295.
[46] M.A. Meyers et al., Acta Mater. 49 (2001) 4025–4039.
[47] A. Kutsukake et al., Key Eng. Mater. 345–346 (2007) 137–140.
[48] Q. Yu et al., Nature 463 (2010) 335–338.
[49] A.S. Khan et al., Int. J. Plast. 27 (2011) 688–706.